2018

Attaching NorA efflux pump inhibitors to methylene blue enhances antimicrobial photodynamic inactivation of Escherichia coli and Acinetobacter baumannii in vitro and in vivo

Ardeshir Rineh
University of Wollongong, arineh@uow.edu.au

John B. Bremner
University of Wollongong, jbremner@uow.edu.au

Michael R. Hamblin
Harvard Medical School, Boston, Massachusetts General Hospital, Harvard-MIT Division of Health Sciences and Technology, hamblin@helix.mgh.harvard.edu

Anthony R. Ball
Gliese 623B

George P. Tegos
Gliese 623B, gtegos@partners.org

See next page for additional authors

Publication Details

Rineh, A., Bremner, J. B., Hamblin, M. R., Ball, A. R., Tegos, G. P. & Kelso, M. J. (2018). Attaching NorA efflux pump inhibitors to methylene blue enhances antimicrobial photodynamic inactivation of Escherichia coli and Acinetobacter baumannii in vitro and in vivo. Bioorganic and Medicinal Chemistry Letters, 28 (16), 2736-2740.

Attaching NorA efflux pump inhibitors to methylene blue enhances antimicrobial photodynamic inactivation of Escherichia coli and Acinetobacter baumannii in vitro and in vivo

Abstract
Resistance of bacteria to antibiotics is a public health concern worldwide due to the increasing failure of standard antibiotic therapies. Antimicrobial photodynamic inactivation (aPDI) is a promising non-antibiotic alternative for treating localized bacterial infections that uses non-toxic photosensitizers and harmless visible light to produce reactive oxygen species and kill microbes. Phenothiazinium photosensitizers like methylene blue (MB) and toluidine blue O are hydrophobic cations that are naturally expelled from bacterial cells by multidrug efflux pumps, which reduces their effectiveness. We recently reported the discovery of a NorA efflux pump inhibitor-methylene blue (EPI-MB) hybrid compound INF55-(Ac)en-MB that shows enhanced photodynamic inactivation of the Gram-positive bacterium methicillin-resistant *Staphylococcus aureus* (MRSA) relative to MB, both *in vitro* and *in vivo*. Here, we report the surprising observation that INF55-(Ac)en-MB and two related hybrids bearing the NorA efflux pump inhibitors INF55 and INF271 also show enhanced aPDI activity *in vitro* (relative to MB) against the Gram-negative bacteria *Escherichia coli* and *Acinetobacter baumannii*, despite neither species expressing the NorA pump. Two of the hybrids showed superior effects to MB in murine aPDI infection models. The findings motivate wider exploration of aPDI with EPI-MB hybrids against Gram-negative pathogens and more detailed studies into the molecular mechanisms underpinning their activity.

Disciplines
Medicine and Health Sciences

Publication Details
Rineh, A., Bremner, J. B., Hamblin, M. R., Ball, A. R., Tegos, G. P. & Kelso, M. J. (2018). Attaching NorA efflux pump inhibitors to methylene blue enhances antimicrobial photodynamic inactivation of Escherichia coli and Acinetobacter baumannii in vitro and in vivo. Bioorganic and Medicinal Chemistry Letters, 28 (16), 2736-2740.

Authors
Ardeshir Rineh, John B. Bremner, Michael R. Hamblin, Anthony R. Ball, George P. Tegos, and Michael J. Kelso

Attaching NorA Efflux Pump Inhibitors to Methylene Blue Enhances Antimicrobial Photodynamic Inactivation of *Escherichia coli* and *Acinetobacter baumannii in vitro* and *in vivo*

Ardeshir Rineh[a], John B. Bremner[a], Michael R. Hamblin[b,c,d], Anthony R. Ball[e], George P. Tegos[e], Michael J. Kelso[a*]

[a]*School of Chemistry and Illawarra Health and Medical Research Institute, University of Wollongong, Wollongong, New South Wales 2522, Australia;* [b]*The Wellman Center for Photomedicine, Massachusetts General Hospital, Boston, Massachusetts 02114, USA;* [c]*Department of Dermatology, Harvard Medical School, Boston, Massachusetts 02114, USA;* [d]*Harvard-MIT Division of Health Sciences and Technology, Cambridge, Massachusetts 02114, USA;* [e]*Gliese 623B, Lowell, Massachusetts 01852, United States.*

*To whom correspondence should be addressed. Email: mkelso@uow.edu.au, Tel.: +61 (0)2 4221 5085, Fax: +61 (0)2 4221 4287

Keywords: Antimicrobial Photodynamic Inactivation, Efflux Pump Inhibitor, Methylene Blue, *Escherichia coli*, *Acinetobacter baumannii*

Abbreviations: Antimicrobial photodynamic inactivation (aPDI), methylene blue (MB), efflux pump inhibitor-methylene blue hybrid (EPI-MB), methicillin-resistant *Staphylococcus aureus* (MRSA), antimicrobial photodynamic inactivation (aPDI), photosensitizing dye (PS), reactive oxygen species (ROS), hydroxyl radicals (•OH), bioluminescent enteropathogenic *E. coli* (EPEC), brain heart infusion (BHI), Cremophor EL (CrEL), colony forming units (CFU) national institutes of health (NIH), relative luminescence units (RLU), resistance nodulation division (RND).

Abstract

Resistance of bacteria to antibiotics is a public health concern worldwide due to the increasing failure of standard antibiotic therapies. Antimicrobial photodynamic inactivation (aPDI) is a promising non-antibiotic alternative for treating localized bacterial infections that uses non-toxic photosensitizers and harmless visible light to produce reactive oxygen species and kill microbes. Phenothiazinium photosensitizers like methylene blue (MB) and toluidine blue O are hydrophobic cations that are naturally expelled from bacterial cells by multidrug efflux pumps, which reduces their effectiveness. We recently reported the discovery of a NorA efflux pump inhibitor-methylene blue (EPI-MB) hybrid compound INF55-(Ac)en−MB that shows enhanced photodynamic inactivation of the Gram-positive bacterium methicillin-resistant *Staphylococcus aureus* (MRSA) relative to MB, both *in vitro* and in *vivo*. Here, we report the surprising observation that INF55-(Ac)en−MB and two related hybrids bearing the NorA efflux pump inhibitors INF55 and INF271 also show enhanced aPDI activity *in vitro* (relative to MB) against the Gram-negative bacteria *Escherichia coli* and *Acinetobacter baumannii*, despite neither species expressing the NorA pump. Two of the hybrids showed superior effects to MB in murine aPDI infection models. The findings motivate wider exploration of aPDI with EPI-MB hybrids against Gram-negative pathogens and more detailed studies into the molecular mechanisms underpinning their activity.

Antibiotic resistance has emerged as a significant threat to global public health,[1-3] with the diminishing treatment options for several infections leading to commentary that we are approaching the end of the 'golden-age' of antibiotics.[4-6] Resistance in the Gram-positive bacteria methicillin resistant *Staphylococcus aureus* (MRSA) is extensive in US hospitals and healthcare facilities,[7] where it accounts for more than 60% of *S. aureus* isolates and kills 23,000 patients each year.[8]

Drug resistant Gram-negative bacteria like *Escherichia coli* and *Acinetobacter baumannii* are increasingly causing life-threatening infections in hospitals,[6, 9, 10] with an estimated 12% of critical infections caused by *E. coli* alone.[11] Data from the Centres for Disease Control and Prevention (CDC) shows that *Acinetobacter baumanii* causes 2% of all nosocomial infections and 7% of infections in critically ill patients on mechanical ventilators.[12] It has been estimated that 63% of the 12,000 annual *Acinetobacter* infections are multidrug resistant and cause 500 deaths annually.

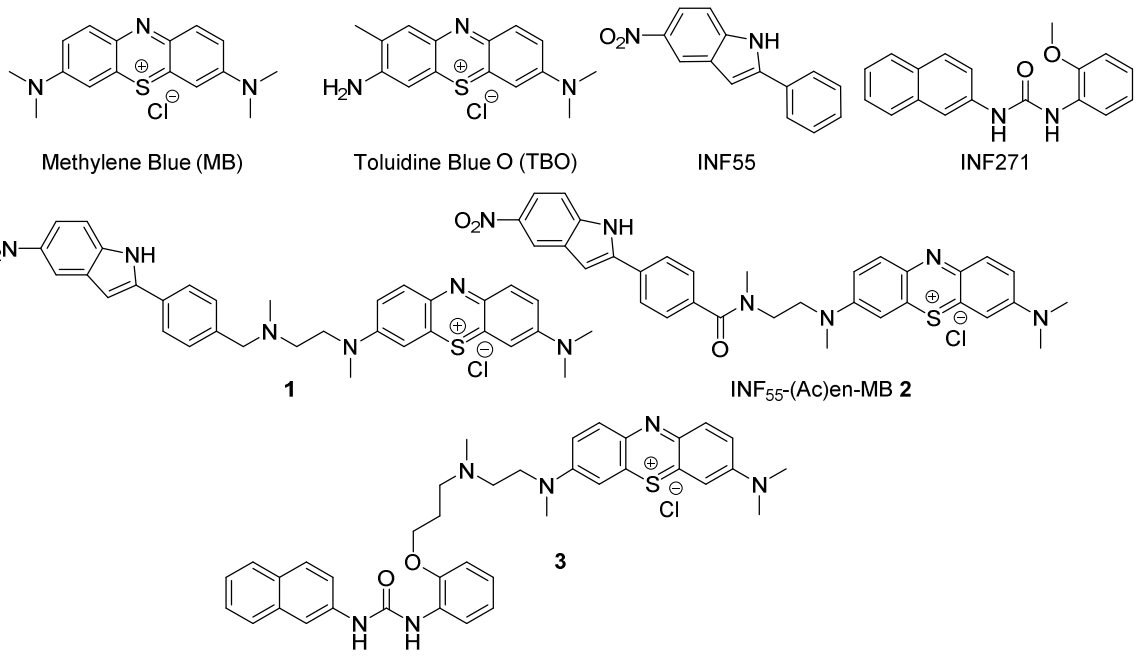

Figure 1. Structures of phenothiazinium photosensitisers methylene blue (MB) and toluidine blue O (TBO) and efflux pump inhibitor-MB hybrids **1-3**. Structures of the NorA efflux pump inhibitors INF55 and INF271[13] are also shown.

Antimicrobial photodynamic inactivation (aPDI) is an emerging non-antibiotic alternative for treating localized infections and countering microbial resistance.[14, 15] In this approach, photosensitizing dyes (PS) like methylene blue (MB) and toluidine blue O (TBO) (Figure 1) are illuminated with red light to produce reactive oxygen species (ROS) (e.g. singlet oxygen, $^1O_2$ and hydroxyl radicals, •OH) that kill microbes.[16, 17] The approach is used routinely in dentistry[18, 19] and in some dermatological treatments.[20, 21]

Over the past ten years the powerful killing effect of aPDI has been demonstrated against a wide variety of Gram-positive and Gram-negative bacteria,[22, 23] with MRSA being the focus of several studies.[24-26] One of the limitations when using phenothiazinium salts in aPDI is that as hydrophobic cations, these photosensitizers are natural substrates for bacterial multi-drug efflux pumps, which serve to rapidly expel the compounds from cells and reduce aPDI effectiveness,[27] presumably by lowering the concentration of intracellular ROS. It was shown that aPDI with phenothiazinium salts can be enhanced in *S. aureus* when used in combination with NorA efflux pump inhibitors (EPI).[28] Based on these observations, we postulated that covalently linking NorA inhibitors to a phenothiazinium PS to form a single EPI-MB hybrid compound might have similar effects, and we recently prepared sixteen such hybrids and reported their aPDI activities against *S. aureus*.[29] Two of the hybrids incorporating the NorA EPI INF55 (**1** and **2**) and one containing the NorA EPI INF271 **3** showed the highest *in vitro* aPDI of MRSA *in vitro*. The most potent hybrid **2** (denoted INF55-(Ac)en−MB) showed enhanced aPDI activity and wound healing effects (relative to MB) in a murine MRSA wound infection model. In the current study, we examined the *in*

vitro and *in vivo* aPDI activities of EPI-MB hybrids **1-3** against two representative Gram-negative bacteria, *E. coli* and *A. baumannii*.

***In vitro* aPDI**

E. coli wild-type (K-12) cells and an isogenic TolC efflux pump knock-out strain JW5503-1 (TolC-) were incubated with MB and hybrids **1-3** over the concentration range 1-20 μM and illuminated with red light (652 nm) at 6 J/cm^2. CFUs were counted from serially diluted aliquots and the results plotted as survival fractions verses compound concentration (Figure 2). MB and the hybrids showed no killing effect against either strain in the dark (Supplementary Data Figure S1 and S2). For the wild-type strain, illumination in the presence of MB produced a 2log$_{10}$ kill at 10 μM, which increased to 2.5log$_{10}$ at 20 μM. MB showed similar killing at 10 μM against the TolC mutant strain with higher killing (3.5 log$_{10}$) at 20 μM. The increased susceptibility of the TolC- mutant was consistent with MB serving as a TolC efflux substrate.[30] Hybrid **1** produced a 2log$_{10}$ kill against the wild-type strain at 10 μM and a 4log$_{10}$ kill at 20 μM. Against the TolC- strain, hybrid **1** produced a 2log$_{10}$ kill at 10 μM that increased to 7log$_{10}$ at 20 μM. For hybrid **2**, a 4log$_{10}$ kill was observed against the wild-type strain at 10 μM, which increased to 6log$_{10}$ at 20 μM. Exceptional potency was seen with **2** against the TolC- strain, where a 6log$_{10}$ kill was observed at 10 μM and almost complete eradication was achieved at 20 μM. Hybrid **3** produced a 3log$_{10}$ kill at the highest concentration (20 μM) against the wild-type strain and 4.5log$_{10}$ against the TolC- mutant. The increased activity of all three hybrids against the TolC- strain relative to the wild-type suggests they may be substrates for this pump.

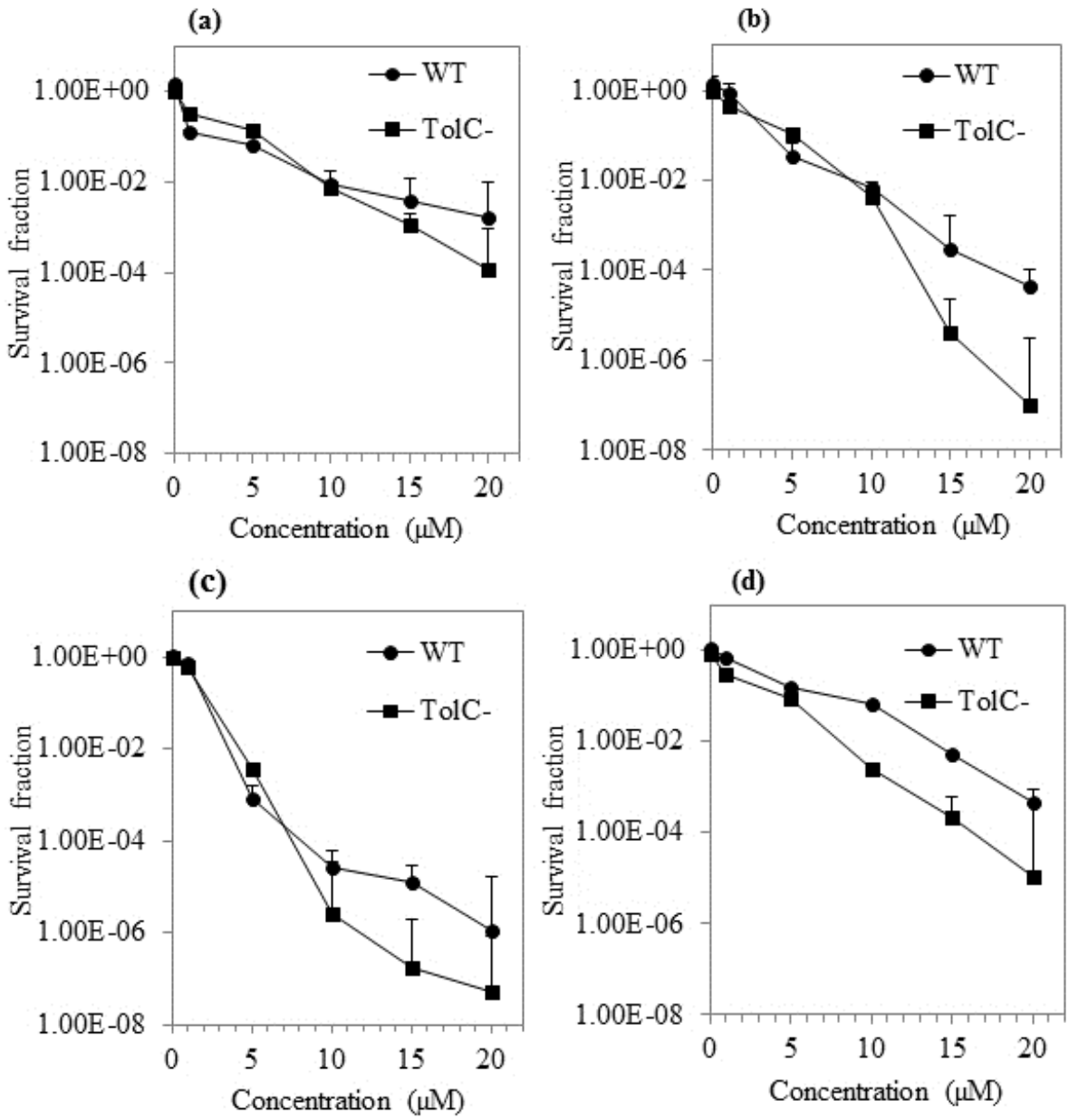

Figure 2. aPDI of *E. coli* wild-type (WT, K-12) and TolC knockout (TolC-, JW5503-1) strains using: (a) MB, (b) **1**, (c) **2** and (d) **3**. Cells were illuminated with 100 mW/cm^2 red light (652 nm, 6 J/cm^2) and survival fractions determined. Data represent the mean ± SEM from three independent experiments.

aPDI of *A. baumannii* was examined *in vitro* using the wild-type strain AB007. MB and the three hybrids showed no killing of AB007 in the dark over the concentration range 1-

20 µM (Figure 3). Following illumination, hybrids **2** and **3** showed similar aPDI potency to MB at 20 µM (~4$\log_{10}$ kill), with hybrid **1** producing an extra $\log_{10}$ kill at this concentration.

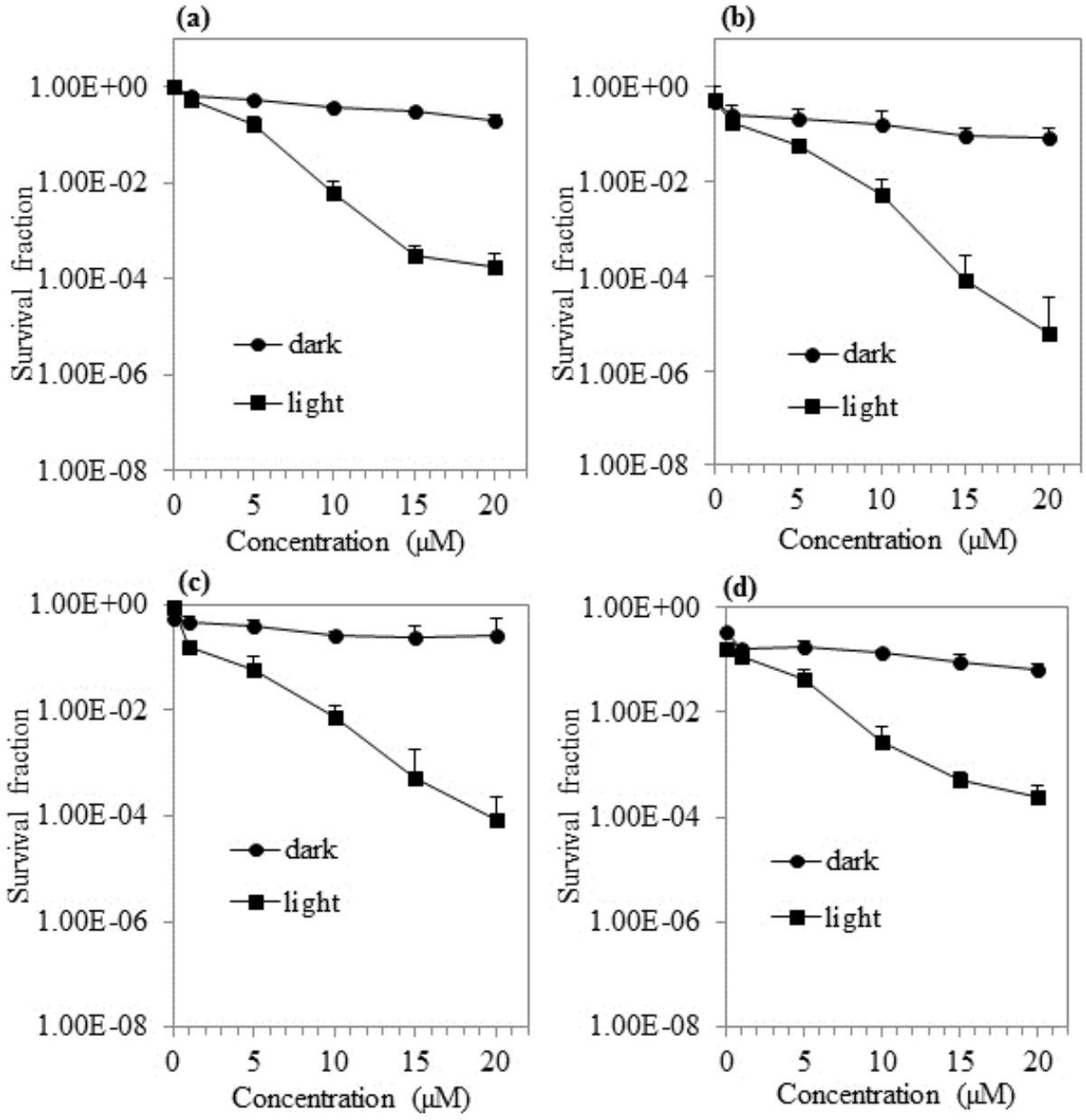

Figure 3. aPDI of *Acinetobacter baumannii* AB007 (and dark controls) using: (a) MB, (b) **1**, (c) **2** and (d) **3** over the concentration range 1-20 µM against. Data represent the mean ± SEM from three independent experiments.

***In vivo* aPDI of *E. coli* with hybrid 2**

Having shown the highest aPDI potency against the two *E. coli* strains *in vitro*, hybrid **2** was evaluated alongside MB for *in vivo* aPDI efficacy using a mouse full-thickness third-degree burn *E. coli* infection model.[31] A pathogenic variant of bioluminescent enteropathogenic *E. coli* (EPEC, WS2572) was inoculated into burns on the shaved dorsal surfaces of mice and the infected areas were treated with solutions containing MB or hybrid **2**. The areas were illuminated with 652 nm red light and luminescence images captured. The normalized luminescence emanating from wounds (relative luminescence units, RLU) during the 'light treatment' phase of the experiment was plotted as a function of applied light fluence (Figure 4(a)).

The light only control cohort (Group A) showed a slight (~10%) reduction in luminescence following application of the highest fluence (120 J/cm^2). Application of MB in the absence of light (Group B) produced a ~25% reduction in luminescence at the same fluence, while aPDI with MB (Group C) resulted in a ~90% reduction in luminescence. In the absence of light, hybrid **2** (Group D) showed a slightly higher killing than MB (~40% reduction in luminescence), while aPDI with hybrid **2** (Group E) produced a remarkable ~80% reduction in bacterial luminescence at low fluence (36 J/cm^2) and total loss of the luminescence signal at 84 J/cm^2.

Post-treatment monitoring of infection sites by capturing daily bioluminescence images for 14 days (Figure 4(b)) revealed a slight rebound in bacterial load for the controls (Group A) and MB treated groups (Groups B and C) 1 day after infection/treatment. Infections in the control groups A, B and D were all resolved (i.e. no luminescence detected) within 13-14 days, while for the MB aPDI cohort (Group C) infections were resolved after 12 days. aPDI with hybrid **2** (Group E) produced a lower bacterial burden compared to all other

groups throughout the entire monitoring period and the infections were resolved more rapidly (10 days).

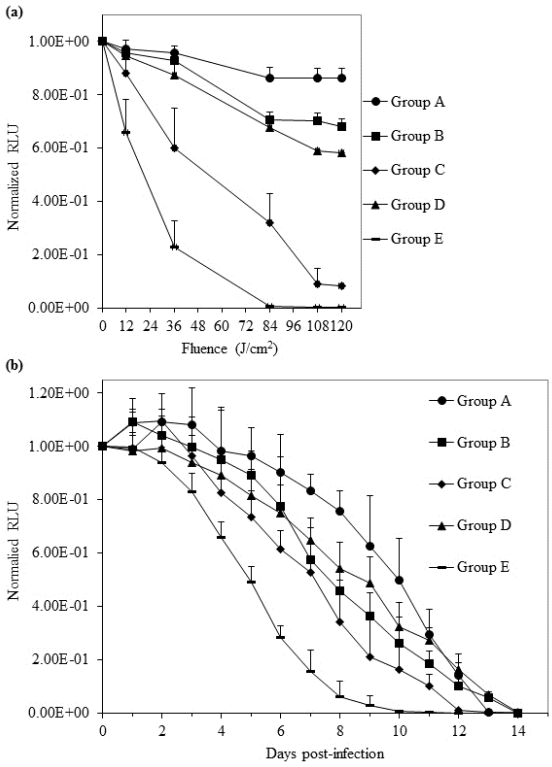

Figure 4. (a) Bioluminescence of *E. coli*-infected mouse burn wounds during initial 'light-treatment' phase of experiment: Group A - light controls (no compound), Group B - MB dark control, Group C - MB with aPDI, Group D - hybrid **2** dark control and Group E - hybrid **2** with aPDI. MB or hybrid (40 µL of 250 µM stock solution) was applied to infection sites. Data represent the mean (± SEM) normalized relative luminescence units (RLU) emanating from the burn wounds of 4-6 mice in each group during application of 0, 12, 36, 84, 108 and 120 J/cm^2 red light (652 nm). (b) Fourteen day post-treatment monitoring of burn wound infection site luminescence.

***In vivo* aPDI of *A. baumannii* with hybrid 1**

Hybrid **1** was tested for *in vivo* aPDI efficacy alongside MB using a mouse needle back-scratch wound abrasion *A. baumannii* infection model.[32] Bioluminescent *A. baumannii* (strain AB Iraqi 007) was inoculated into needle-scratch wounds on the shaved dorsal surfaces of mice and the infected areas were treated with solutions containing MB or hybrid **1**. Control and aPDI treatment groups (Groups A-E) and infection site monitoring were as for the *E. coli* burn model.

The light only controls (Group A) showed no reduction in the luminescence signal over the 20 min 'light-treatment' phase of the experiment, confirming that the *A. baumannii* infection was stable over this period (Figure 5(a)). The MB (Group B) and hybrid **1** (Group D) dark controls produced slight reductions (<25%) in luminescence during this period. A 50% reduction in the luminescence signal was seen following aPDI with MB (Group C) at 36 J/ cm^2 and total loss of the signal occurred at 108 J/cm^2. aPDI with hybrid **1** (Group E) showed an impressive 95% reduction in luminescence at low fluence (36 J/cm^2) and complete loss of the signal at 84 J/cm^2.

A rebound in bacterial load (50% or greater) was observed 1 day after infection/treatment in all cohorts except Group E (aPDI with **1**) (Figure 5(b)). Low level luminescence remained in control Group A at Day 14, while the signal disappeared after 12 days in the presence of MB in the dark (Group B). aPDI with MB (Group C) produced slightly lower bacterial loads throughout the monitoring period and the luminescence signal had disappeared after 10 days. Treatment with hybrid **1** in the dark (Group D) reduced the bacterial load at a rate that paralleled the MB dark control, with infections resolving within 12 days. aPDI with **1** (Group E) showed lower bacterial loads than all other cohorts throughout the entire monitoring period and the infections were resolved within 6 days.

Bioluminescence images captured from representative animals in Groups A-E during the first 6 days of the monitoring period are provided in the Supplementary Data (Figure S3).

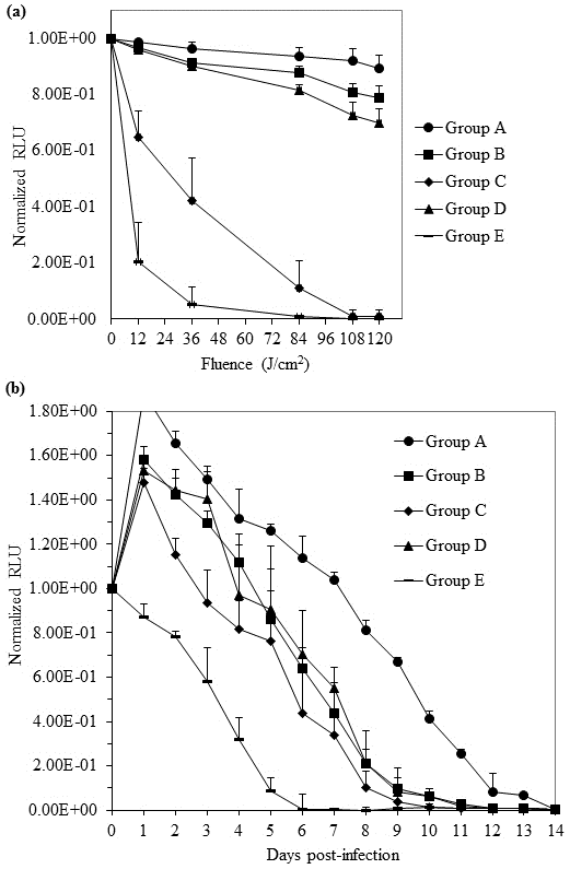

Figure 5. (a) Bioluminescence of *A. baumannii*-infected mouse back scratch abrasion wounds during initial 'light-treatment' phase of experiment: Group A - light control (no compound), Group B - MB dark control, Group C - MB with aPDI, Group D - hybrid **1** dark control and Group E - hybrid **1** with aPDI. MB or hybrid (40 µL of a 250 µM stock solution) was applied to infection sites. Data represent the mean (± SEM) normalized relative luminescence units (RLU) emanating from the scratch wounds of 4-6 mice in each group after application of 0, 12, 36, 84, 108 and 120 J/cm^2 red light (652 nm). (b) Fourteen day post-treatment monitoring of wound infection site luminescence.

Previous work by Tegos *et al.* showed that phenothiazinium-based photosensitizers such as MB are substrates for bacterial MDR efflux pumps and that these pumps can expel photosensitizers from cells leading to reduced aPDI effectiveness.[27] They also showed that aPDI with MB against the Gram-positive bacterium *S. aureus* is enhanced by the co-presence of inhibitors of the major facilitator efflux pump NorA.[27] We recently reported that synthetic hybrids formed by covalently attaching NorA pump inhibitors to MB also enhance aPDI of *S. aureus*,[29] with three leading hybrids **1**-**3** showing significant ROS generation upon illumination, potent aPDI of *S. aureus in vitro* and higher intracellular accumulation in *S. aureus* cells than MB. When hybrid **2** (INF55-(Ac)en–MB) was advanced to *in vivo* aPDI studies it outperformed MB by all measures in a murine back-scratch *S. aureus* infection model.

Buoyed by these findings, we chose to study the aPDI effects of **1-3** against two representative Gram-negative bacteria, i.e. *E. coli* and *A. baumannii*, despite neither having previously been shown to express membrane efflux pumps that are inhibited by INF55 or INF271. Indeed these two EPIs to date have only been shown to inhibit the NorA pump in *S. aureus*.[33] Nevertheless, Gram-negative bacteria are known to be less susceptible to extracellular singlet oxygen than Gram-positive species,[34,35] suggesting that a hybrid approach that could increase intracellular ROS was worth investigating.

The major efflux pump in *E. coli* comprises the outer membrane channel protein TolC and two other proteins AcrA and AcrB, which together form the tripartite efflux system AcrAB-TolC; a member of the resistance nodulation division (RND) superfamily.[36] Several reports have shown that phenothiazinium salts are efflux substrates in *E. coli*.[27,37,38] When tested against *E. coli* wild-type cells and a TolC knockout mutant, all three hybrids showed greater aPDI than MB against both strains. When the most potent hybrid **2** was evaluated for aPDI efficacy in a murine *E. coli* burn infection model it showed greater aPDI than MB during the

'light-treatment' phase of the experiment, lower bacterial counts throughout the post-treatment monitoring period and more rapid resolution of the infection. These results suggest that hybrid **2** is either a poorer substrate for *E. coli* pumps than MB or it acts directly as a pump inhibitor, both of which would lead to higher intracellular concentrations of the hybrid and higher intracellular ROS during aPDI. Further experiments are ultimately required, however, to confirm which (if any) *E. coli* pumps are targeted by **2**, how they are affected and whether these effects play a dominant role in the enhanced *E. coli* aPDI seen with **2**.

The most prevalent pumps in *A. baumannii* are members of the RND superfamily and include the AdeABC two-component regulatory system AdeIJK and AdeFGH. Non-RND efflux systems have also been characterised in *A. baumannii*.[39] When tested *in vitro* for aPDI of *A. baumannii* AB007, hybrids **2** and **3** showed no increase in activity relative to MB. However, hybrid **1** showed $1\log_{10}$ greater killing than MB at the highest concentration (20 μM) and was subsequently found to outperform MB in a murine aPDI *A. baumannii* infection model. These results are consistent with **1** (but not **2** or **3**) being a poorer efflux substrate than MB in *A. baumannii* and possibly a pump inhibitor, although alternative explanations are plausible. For example, the physicochemical properties of **1** may engender higher affinity for *A. baumannii* cell surface components relative to MB and **2/3**, leading to higher cell-localized concentrations of ROS during aPDI and greater lethality. The relationship between higher cell surface affinity of photosensitizers and increased aPDI has been noted.[40]

In conclusion, this study demonstrates that attaching NorA EPIs to MB can increase aPDI effectiveness against the Gram-negative pathogens *E. coli* and *A. baumannii in vitro* and *in vivo*. Further experiments to establish whether INF55, INF271 and the hybrids are inhibitors of efflux pumps in Gram-negative bacteria will shed light on the underlying mechanisms responsible for the observed increases in aPDI efficacy relative to MB. Hybrids

containing MB attached to known inhibitors of Gram-negative efflux pumps (e.g. Phenyl-arginine-beta-naphthylamide, PaβN)[41] would be of interest in future studies.

Acknowledgements

We thank the University of Wollongong (Wollongong, Australia) and Massachusetts General Hospital (Boston, USA) for supporting this work. The study was partially funded by the US NIH (R01 AI076372 to J.B.B. and M.J.K.; AI050875 to M.R.H.).

Supplementary Data

Supplementary data associated with this article can be found, in the online version, at XXXXX

References and notes

1. Ciorba V, Odone A, Veronesi L, Pasquarella C, Signorelli C. Antibiotic resistance as a major public health concern: epidemiology and economic impact. *Annali Di Igiene: medicina preventiva e di comunita*. 2015;27:562.
2. Roca I, Akova M, Baquero F, et al. The global threat of antimicrobial resistance: science for intervention. *New Microbes New Infect*. 2015;6:22.
3. Prestinaci F, Pezzotti P, Pantosti A. Antimicrobial resistance: A global multifaceted phenomenon. *Pathog Glob Health*. 2015;109:309.
4. Spellberg B, Gilbert DN. The future of antibiotics and resistance: A tribute to a career of leadership by John Bartlett. *Clin Infect Dis*. 2014;59:S71.
5. Spellberg B. The future of antibiotics. *Crit Care*. 2014;18:228.
6. Li XZ, Plésiat P, Nikaido H. The challenge of efflux-mediated antibiotic resistance in gram-negative bacteria. *Clin Microbiol Rev*. 2015;28:337.
7. Rossolini GM, Arena F, Pecile P, Pollini S. Update on the antibiotic resistance crisis. *Curr Opin Pharmacol*. 2014;18:56.
8. CDC. Centers for Disease Control and Prevention, Office of Infectious Disease Antibiotic resistance threats in the United States; 2013. https://www.cdc.gov/drugresistance/threat-report-2013/index.html. Accessed April 10, 2017.
9. Nikaido H, Vaara M. Molecular basis of bacterial outer membrane permeability. *Microbiol Rev*. 1985;49:1.
10. Mehrad B, Clark NM, Zhanel GG, Lynch JP. Antimicrobial resistance in hospital-acquired gram-negative bacterial infections. *Chest*. 2015;147:1413.
11. Sievert DM, Ricks P, Edwards JR, et al. Antimicrobial-resistant pathogens associated with healthcare-associated infections: summary of data reported to the National Healthcare Safety Network at the Centers for Disease Control and Prevention, 2009-2010. *Infect Control Hosp Epidemiol*. 2013;34:1.

12. CDC. Acinetobacter in Healthcare Settings; 2010. https://www.cdc.gov/hai/organisms/acinetobacter.html. Accessed April 10, 2017.
13. Markham PN, Westhaus E, Klyachko K, Johnson ME, Neyfakh AA. Multiple novel inhibitors of the NorA multidrug transporter of *Staphylococcus aureus*. *Antimicrob Agents Chemother*. 1999;43:2404.
14. Wainwright M. Photodynamic antimicrobial chemotherapy (PACT). *J Antimicrob Chemother*. 1998;42:13.
15. Zeina B, Greenman J, Purcell WM, Das B. Killing of cutaneous microbial species by photodynamic therapy. *Br J Dermatol*. 2001;144:274.
16. Dai T, Huang YY, Hamblin MR. Photodynamic therapy for localized infections - state of the art. *Photodiagnosis Photodyn Ther*. 2009;6:170.
17. Castano AP, Demidova TN, Hamblin MR. Mechanisms in photodynamic therapy: part one - photosensitizers, photochemistry and cellular localization. *Photodiagnosis Photodyn Ther*. 2004;1:279.
18. Wilson M. Bactericidal effect of laser light and its potential use in the treatment of plaque-related diseases. *Int Dent J*. 1994;44:181.
19. Wilson M. Photolysis of oral bacteria and its potential use in the treatment of caries and periodontal disease. *J Appl Bacteriol*. 1993;75:299.
20. Sperandio FF, Simoes A, Aranha AC, Correa L, Orsini Machado de Sousa SC. Photodynamic therapy mediated by methylene blue dye in wound healing. *Photomed Laser Surg*. 2010;28:581.
21. Choudhary S, Nouri K, Elsaie ML. Photodynamic therapy in dermatology: a review. *Lasers Med Sci*. 2009;24:971.
22. Fotinos N, Convert M, Piffaretti JC, Gurny R, Lange N. Effects on gram-negative and gram-positive bacteria mediated by 5-aminolevulinic acid and 5-aminolevulinic acid derivatives. *Antimicrob Agents Chemother*. 2008;52:1366.
23. Schastak S, Ziganshyna S, Gitter B, Wiedemann P, Claudepierre T. Efficient photodynamic therapy against gram-positive and gram-negative bacteria using THPTS, a cationic photosensitizer excited by infrared wavelength. *PLoS One*. 2010;5 e11674,1.
24. Ferro S, Ricchelli F, Monti D, Mancini G, Jori G. Efficient photoinactivation of methicillin-resistant *Staphylococcus aureus* by a novel porphyrin incorporated into a poly-cationic liposome. *Int J Biochem Cell Biol*. 2007;39:1026.
25. Nitzan Y, Gozhansky S, Malik Z. Effect of photoactivated hematoporphyrin derivative on the viability of *Staphylococcus aureus*. *Curr Microbiol*. 1983;8:279.
26. Fu X, Fang Y, Yao M. Antimicrobial photodynamic therapy for methicillin-resistant *Staphylococcus aureus* infection. *BioMed Res Int*. 2013;2013.
27. Tegos GP, Hamblin MR. Phenothiazinium antimicrobial photosensitizers are substrates of bacterial multidrug resistance pumps. *Antimicrob Agents Chemother*. 2006;50:196.
28. Tegos GP, Masago K, Aziz F, Higginbotham A, Stermitz FR, Hamblin MR. Inhibitors of bacterial multidrug efflux pumps potentiate antimicrobial photoinactivation. *Antimicrob Agents Chemother*. 2008;52:3202.
29. Rineh A, Dolla NK, Ball AR, et al. Attaching the NorA efflux pump inhibitor INF55 to methylene blue enhances antimicrobial photodynamic inactivation of methicillin-resistant *Staphylococcus aureus* in vitro and in vivo. *ACS Infect Dis*. 2017;3:756.
30. Yu QZEW. Microbial efflux pumps. Norfolk, UK: Caister Academic Press; 2013.
31. Huang L, Wang M, Dai T, et al. Antimicrobial photodynamic therapy with decacationic monoadducts and bisadducts of [70]fullerene: in vitro and in vivo studies. *Nanomedicine* (London, England). 2014;9:253.

32. Dai T, Tegos GP, Zhiyentayev T, Mylonakis E, Hamblin MR. Photodynamic therapy for methicillin-resistant *Staphylococcus aureus* infection in a mouse skin abrasion model. *Lasers Surg Med*. 2010;42:38.
33. Tegos G, Stermitz FR, Lomovskaya O, Lewis K. Multidrug pump inhibitors uncover remarkable activity of plant antimicrobials. *Antimicrob Agents Chemother*. 2002;46:3133.
34. Huang L, Xuan Y, Koide Y, Zhiyentayev T, Tanaka M, Hamblin MR. Type I and Type II mechanisms of antimicrobial photodynamic therapy: An *in vitro* study on Gram-negative and Gram-positive bacteria. *Lasers Surg Med*. 2012;44:490.
35. Valduga G, Bertoloni G, Reddi E, Jori G. Effect of extracellularly generated singlet oxygen on gram-positive and gram-negative bacteria. *J Photochem Photobiol B, Biology*. 1993;21:81.
36. Koronakis V. TolC - the bacterial exit duct for proteins and drugs. *FEBS Letters*. 2003;555:66.
37. Minnock A, Vernon DI, Schofield J, Griffiths J, Parish JH, Brown SB. Mechanism of uptake of a cationic water-soluble pyridinium zinc phthalocyanine across the outer membrane of *Escherichia coli*. *Antimicrob Agents Chemother*. 2000;44:522.
38. Molnar J, Hever A, Fakla I, Fischer J, Ocsovski I, Aszalos A. Inhibition of the transport function of membrane proteins by some substituted phenothiazines in *E. coli* and multidrug resistant tumor cells. *Anticancer Res*. 1997;17:481.
39. Coyne S, Courvalin P, Perichon B. Efflux-mediated antibiotic resistance in Acinetobacter spp. *Antimicrob Agents Chemother*. 2011;55:947.
40. Hamblin MR, O'Donnell DA, Murthy N, et al. Polycationic photosensitizer conjugates: effects of chain length and gram classification on the photodynamic inactivation of bacteria. *J Antimicrob Chemother*. 2002;49:941.
41. Pannek S, Higgins PG, Steinke P, et al. Multidrug efflux inhibition in *Acinetobacter baumannii*: comparison between 1-(1-naphthylmethyl)-piperazine and phenyl-arginine-beta-naphthylamide. *J Antimicrob Chemother*. 2006;57:970.

Supplementary Data

Attaching NorA Efflux Pump Inhibitors to Methylene Blue Enhances Antimicrobial Photodynamic Inactivation of *Escherichia coli* and *Acinetobacter baumanii in vitro* and *in vivo*

Ardeshir Rineh[a], John B. Bremner[a], Michael R. Hamblin[b,c,d], Anthony R. Ball[e], George P. Tegos[e], Michael J. Kelso[a*]

[a]*School of Chemistry and Illawarra Health and Medical Research Institute, University of Wollongong, Wollongong, New South Wales 2522, Australia;* [b]*The Wellman Center for Photomedicine, Massachusetts General Hospital, Boston, Massachusetts 02114, USA;* [c]*Department of Dermatology, Harvard Medical School, Boston, Massachusetts 02114, USA;* [d]*Harvard-MIT Division of Health Sciences and Technology, Cambridge, Massachusetts 02114, USA;* [e]*Gliese 623B, Lowell, Massachusetts 01852, United States.*

Table of Contents

(1) Microbial strains and culture conditions. *E. coli* K-12 was used as the wild type strain. *E. coli* JW5503-1 from Dr. Michael LaFleur's laboratory (Northeastern University) was used as the TolC knock out mutant (TolC-). The bioluminescent enteropathogenic *E. coli* (EPEC) strain WS2572 (Xenogen, Inc., now called Caliper Life Sciences Inc., Hopkinton, MA) was used for *in vivo* studies. *Acinetobacter baumannii* AB007 was used for *in vitro* studies and *A. baumannii* bioluminescence AB Iraqi 007 strain was used for *in vivo* studies. A list of these strains and strain identifiers is provided in Table S1. All cells were cultured under standard conditions in brain heart infusion (BHI) media (Fisher Scientific, Braintree, MA, USA) with aeration at 37 °C. Cells were used at 10^7-10^8 CFU per mL (mid-log growth phase) in all experiments.

(2) Photosensitizers and light sources. Hybrids **1-3** were synthesised as described previously.[1] Stock solutions of MB and hybrids were prepared as Cremophor EL (CrEL, Sigma Aldrich) micellar suspensions diluted in phosphate-buffered saline (PBS) to a final concentration of 200 μM. Solutions were stored for a maximum of 2 weeks at 4 °C in the dark.[1] The light source for illumination was a non-coherent lamp with a 30 nm-band-pass filter 652 ± 15 nm (LC122; LumaCare, London, UK). Total power output from the fibre bundle was 300 mW, with 96-well plates positioned at a height such that 100 mW/cm^2 irradiance was applied.

(3) *In vitro* PDI studies. Bacterial strains (10^7 CFU) were incubated with MB or hybrids at room temperature in 96-well plates at concentrations between 0-20 μM for 30 min before being illuminated with 652 nm light at an energy density of 6 J/cm^2. Cell suspensions were centrifuged at 12,000 rpm and then washed twice with sterile PBS. Aliquots were streaked onto square BHI agar plates after 10-fold serial dilution in PBS (to provide 10^{-1}-10^{-6}

dilutions) and then incubated overnight at 37 °C. Colony forming units (CFU) were counted and survival fractions determined, as described by Jett et al.[2] The same procedures were used for dark controls without application of light.

(4) Mouse full-thickness burn infection model.[3] Animal procedures were approved by the Subcommittee on Research Animal Care (IACUC) at Massachusetts General Hospital (MGH) and performed according to the guidelines of the National Institutes of Health (NIH). Adult female BALB/c mice (aged 6-8 weeks; 17-21 g) were purchased from Charles River Laboratories, (Wilmington, MA). Each animal was housed separately (i.e. one per cage) and maintained on a 12 h light/12 h dark cycle with access to food and water *ad libitum*. A mouse full-thickness burn model was used for studies with *E. coli*. Mice were anesthetized using a ketamine-xylazine cocktail injected intraperitoneally (i.p.) and the dorsal surface was shaved. Two preheated (95 °C) brass blocks (Small Parts Inc., Miami, FL) were held for 10 s against the opposing sides of an elevated skin fold on the dorsal surface to create a non-lethal, full-thickness third-degree burn.[4] To relieve pain, each mouse received buprenorphine (0.03 mg/kg subcutaneously twice a day) for 3 days after burn creation. The procedure produced 15 mm x 10 mm (150 mm^2) burn areas corresponding to 4% of the total body surface area.[5] To avoid dehydration, mice received i.p. injections of 0.5 mL sterile saline (Phoenix Scientific Inc., St. Joseph, MO) immediately after burning. Five minutes later, a 50 µL aliquot of bioluminescent *E. coli* EPEC WS2572 (Xen14) cells in sterile PBS (10^8 CFU/mL) was inoculated onto the burn surface using a pipette tip.[6] Luminescence images from the burns were captured immediately after inoculation and at intervals thereafter (see text).

(5) Mouse needle scratch infection model.[7] Mice were immunosuppressed with two intraperitoneal (i.p.) cyclophosphamide injections, the first administered 4 days prior to

inoculation (150 mg/kg i.p.) and the second (100 mg/kg i.p.) one day prior. On the day of inoculation (Day 0), mice were anesthetized with i.p. injections of a ketamine (100 mg/kg)/xylazine (10mg/kg) cocktail and their dorsal surfaces were shaved. A 28-gauge needle (Micro-Fine IV, Becton Dickinson, Franklin Lakes, NJ) was used to scratch 6 x 6 cross-hatch lines 1.5 mm apart in a square covering ~1.0 cm^2 on the dorsal surfaces to create a skin abrasion wound.[7,8] The scratches were carefully applied so that only the stratum corneum and upper-layer of the epidermis were damaged. Five minutes after wounding a 40 μL aliquot was drawn from a 10^8 CFU/mL suspension of *A. baumannii* in PBS and spread evenly over the wound area using a micropipette tip. Bioluminescence images were captured immediately after inoculation and at intervals thereafter (see text).

Thirty minutes after inoculation (both burn and wound models), 40 μL of a 250 μM stock solution of MB or hybrid was applied to the infection site and a second bioluminescence image was captured. Fifteen minutes after compound addition (to allow binding/penetration into cells) a third image was captured (Time = 0). Mice were then illuminated with 652 nm light in aliquots over a 20 min period, corresponding to cumulative fluences of 12, 36, 84, 108 and 120 J/cm^2. Bioluminescence images were captured after each light dose. For the absolute control group (Group A - light only) and dark control groups (Groups B and D), images were captured at the equivalent times post-inoculation. For post-treatment monitoring, bioluminescence images were captured daily for two weeks (Days 1-14).

(6) Bioluminescence imaging. The imaging system consisted of an intensified charge-coupled-device (ICCD) camera (model C2400-30H; Hamamatsu Photonics, Bridgewater, NJ), an imaging box, a camera controller on top of the imaging box, an image processor (C5510-50; Hamamatsu) and a colour monitor (PVM1454Q; Hamamatsu). Light-emitting

diodes were fitted inside the imaging box to provide light for dimensional imaging. With the system in photo-counting mode, images were built at extremely low-light levels by identifying and integrating individual photons emitted. To obtain images, mice were anesthetized by i.p. ketamine-xylazine cocktail injection and placed on an adjustable stage in the specimen chamber such that the infected wounds were located directly under the camera. A grayscale background image of each wound was obtained followed by a photon count for the same region. Using Argus software, the complete photon count was quantified as relative luminescence units (RLUs) and displayed in a false-colour scale ranging from most intense (pink) to least intense (blue).

Table S1. List of bacterial strains.

Entry	Strain	Name and number	Use	Source/reference
1	*A. baumannii*	AB007	*In vitro* and *in vivo*	Ref 9
2	*E. coli*	EC K-12	*in vitro* as wild-type	ATCC PTA-7555/Ref 10
3	*E. coli*	JW5503-1	*in vitro* as TolC knock out (TolC-)	Michael La fleur NEU (from Keio collection)
4	*E. coli*	EPEC WS2572 (XEN14)	*in vivo*	Xenogen Inc

Bioluminescent strains used for *in vivo* studies are highlighted in yellow.

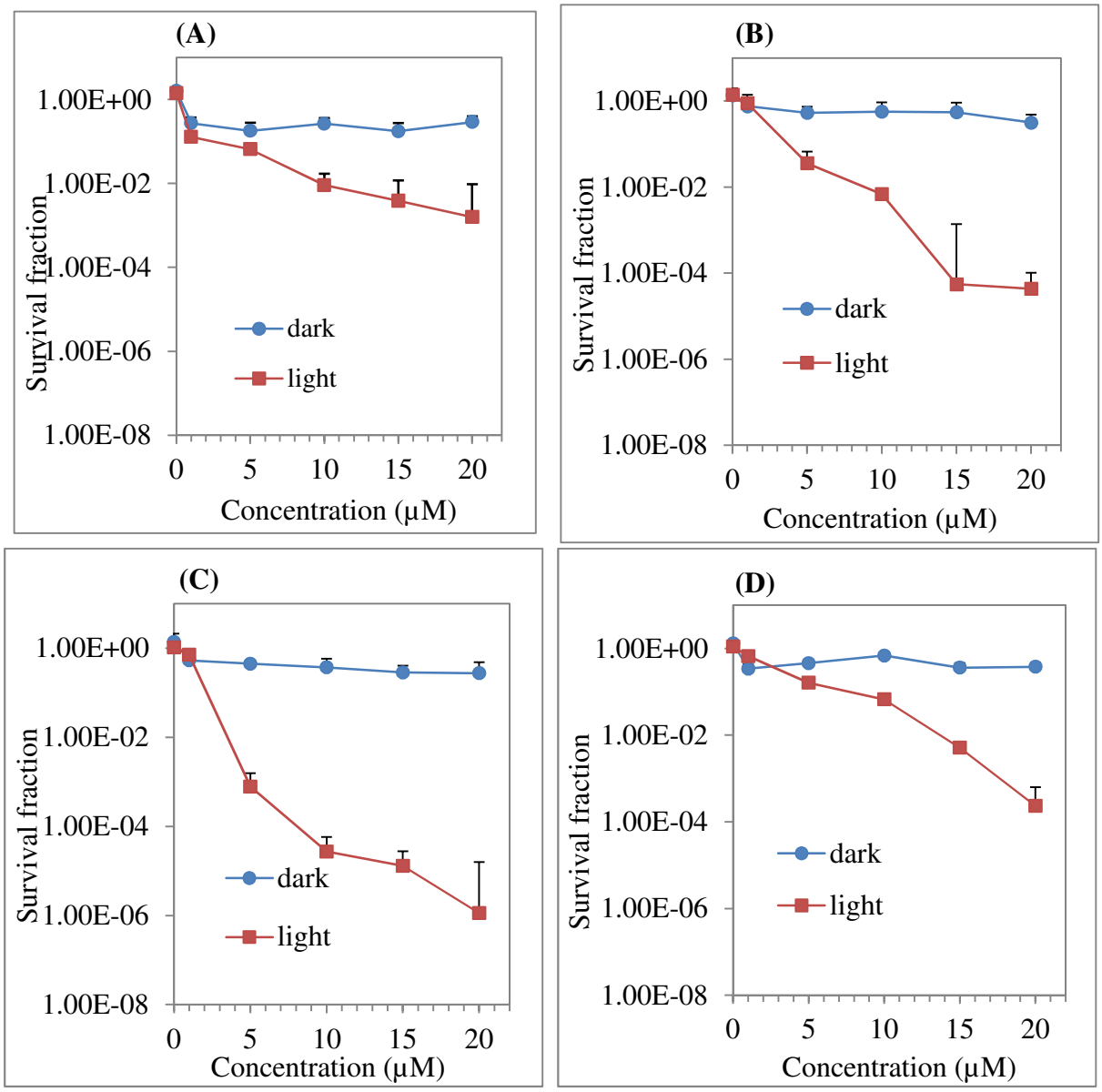

FIG S1. aPDI activity (with dark controls) for: (A) MB (B) **1**, (C) **2** and (D) **3** over the concentration range 1-20 µM against the *E. coli* wild-type strain.

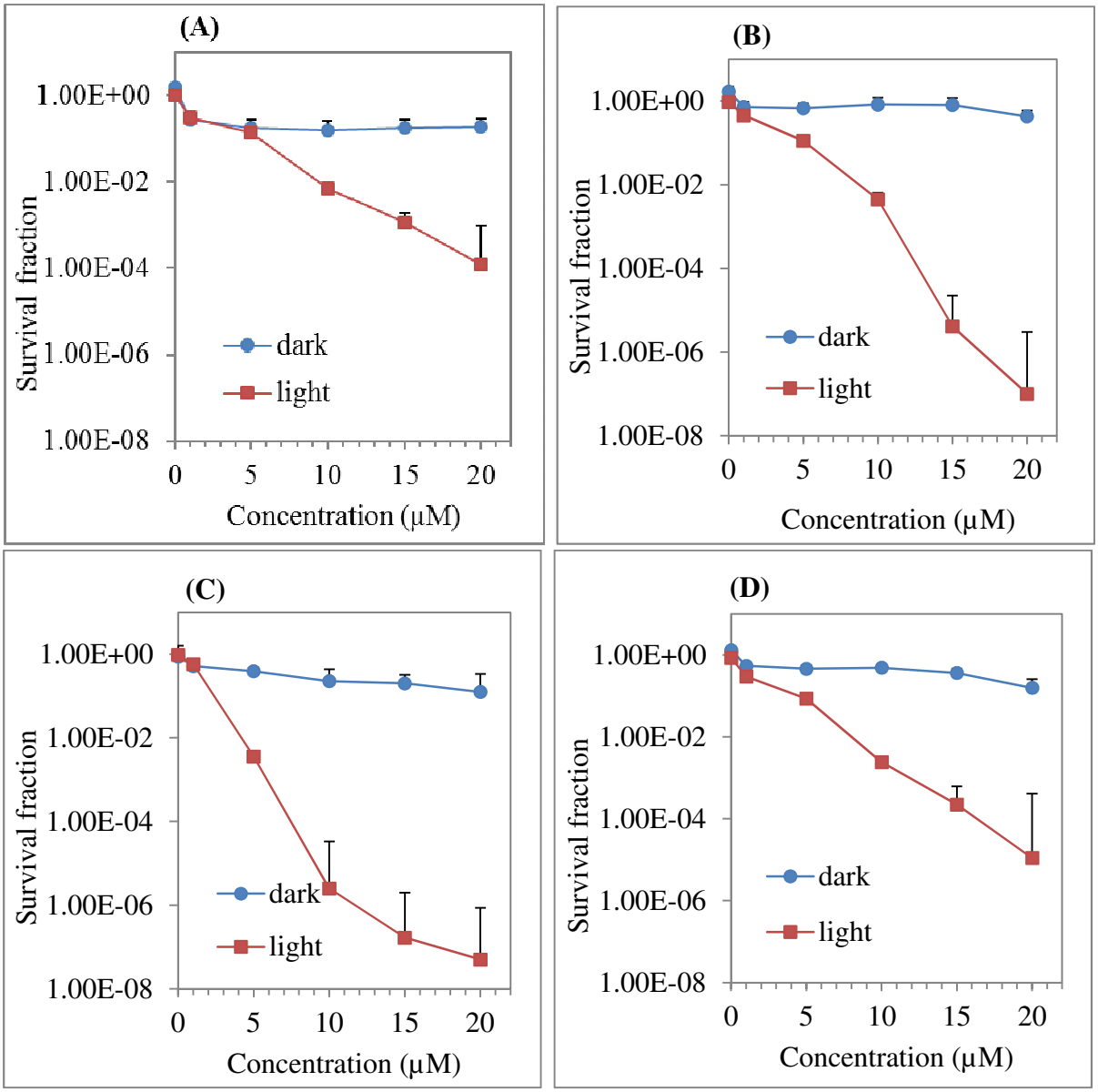

FIG S2. aPDI activity (and dark controls) for (A) MB, (B) **1**, (C) **2** and (D) **3** over the concentration range 1-20 µM against *E. coli* TolC knock out strain JW5503-1.

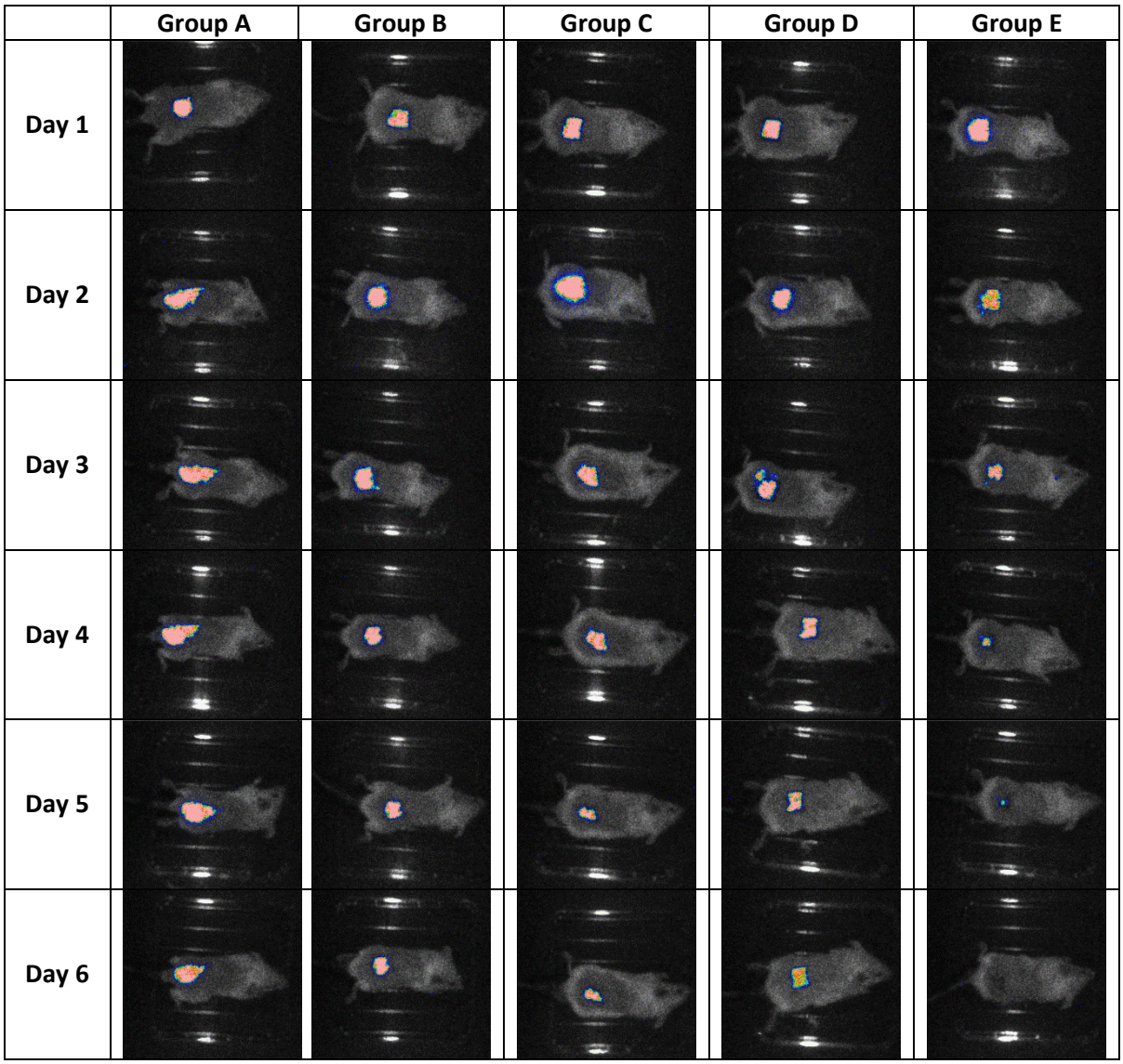

FIG S3. Bioluminescence images captured from representative animals in Groups A-E in the *A. baumannii* needle scratch model. Post-treatment monitoring showed that complete disappearance of luminescence occurred fastest (Day 6) for Group E (aPDI with hybrid **1**).

Supplementary Data References

1. Rineh A, Dolla NK, Ball AR, et al. Attaching the NorA efflux pump inhibitor INF55 to methylene blue enhances antimicrobial photodynamic inactivation of methicillin-resistant *Staphylococcus aureus* in vitro and in vivo. *ACS Infect Dis*. 2017;3:756.
2. Jett BD, Hatter KL, Huycke MM, Gilmore MS. Simplified agar plate method for quantifying viable bacteria. *Bitechniques*. 1997;23:648.
3. Dai T, Tegos GP, Lu Z, et al. Photodynamic therapy for *Acinetobacter baumannii* burn infections in mice. *Antimicrob Agents Chemother*. 2009;53:3929.
4. Stevens EJ, Ryan CM, Friedberg JS, Barnhill RL, Yarmush ML, Tompkins RG. A quantitative model of invasive Pseudomonas infection in burn injury. *J Burn Care Rehabil*. 1994;15:232.
5. Gilpin DA. Calculation of a new Meeh constant and experimental determination of burn size. *Burns Incl Therm Inj*. 1996;22:607.
6. Ha U, Jin S. Expression of the soxR gene of *Pseudomonas aeruginosa* is inducible during infection of burn wounds in mice and is required to cause efficient bacteremia. *Infect Immun*. 1999;67:5324.
7. Dai T, Tegos GP, Zhiyentayev T, Mylonakis E, Hamblin MR. Photodynamic therapy for methicillin-resistant *Staphylococcus aureus* infection in a mouse skin abrasion model. *Lasers Surg Med*. 2010;42:38.
8. Dai T, Kharkwal GB, Tanaka M, Huang YY, Bil de Arce VJ, Hamblin MR. Animal models of external traumatic wound infections. *Virulence*. 2011;2:296.
9. Dai T, Tegos GP, Lu Z, et al. Photodynamic Therapy for *Acinetobacter baumannii* Burn Infections in Mice. *Antimicrob Agents Chemother*. 2009;53:3929.
10. Tegos GP, Hamblin MR. Phenothiazinium antimicrobial photosensitizers are substrates of bacterial multidrug resistance pumps. *Antimicrob Agents Chemother*. 2006;50:196.